POST PRINT

Pubblicato da WILEY

https://onlinelibrary.wiley.com/doi/10.1002/jcp.25815

doi: 10.1002/jcp.25815. Epub 2017 Feb 10.

Lipid profiling of *parkin*-mutant human skin fibroblasts

Simona Lobasso[1] | Paola Tanzarella[1] | Daniele Vergara[2] | Michele Maffia[2] | Tiziana Cocco[1] | Angela Corcelli[1]

[1] Department of Basic Medical Sciences, Neurosciences and Sensory Organs, University of Bari "A. Moro", Bari, Italy

[2] Department of Biological and Environmental Sciences and Technologies, University of Salento, Lecce, Italy

Correspondence
Tiziana Cocco and Angela Corcelli, Department of Basic Medical Sciences, Neurosciences and Sensory Organs, University of Bari "A. Moro", pl. G. Cesare 11, I-70124 Bari, Italy.
Email: tizianamaria.cocco@uniba.it (T.C.), angela.corcelli@uniba.it (A.C.)

Funding information
University of Bari "A. Moro", Bari, Italy; Sanofi- Aventis Deutschland GmbH, Frankfurt am Main, Germany

Parkin mutations are a major cause of early-onset Parkinson's disease (PD). The impairment of protein quality control system together with defects in mitochondria and autophagy process are consequences of the lack of parkin, which leads to neurodegeneration. Little is known about the role of lipids in these alterations of cell functions. In the present study, *parkin*-mutant human skin primary fibroblasts have been considered as cellular model of PD to investigate on possible lipid alterations associated with the lack of parkin protein. Dermal fibroblasts were obtained from two unrelated PD patients with different *parkin* mutations and their lipid compositions were compared with that of two control fibroblasts. The lipid extracts of fibroblasts have been analyzed by combined matrix-assisted laser desorption/ionization-time-of-flight mass spec- trometry (MALDI-TOF/MS) and thin-layer chromatography (TLC). In parallel, we have performed direct MALDI-TOF/MS lipid analyses of intact fibroblasts by skipping lipid extraction steps. Results show that the proportions of some phospholipids and glycosphingo- lipids were altered in the lipid profiles of *parkin*-mutant fibroblasts. The detected higher level of gangliosides, phosphatidylinositol, and phosphatidylserine could be linked to dysfunction of autophagy and mitochondrial turnover; in addition, the lysophosphatidylcholine increase could represent the marker of neuroinflammatory state, a well-known component of PD.

KEYW ORDS
fibroblasts, gangliosides, lipidomics, MALDI-TOF/MS, phospholipids

Abbreviations: 9-AA, 9-aminoacridine hemihydrate; CL, cardiolipin; GBA, glucocerebrosidase; Hemi BMP or AcylPG, Hemi Bis (monoacylglycero) phosphate; LPC, lysophosphatidylcholine; MALDI-TOF/MS, matrix-assisted laser desorption/ionization-time-of-flight mass spectrometry; PC, phosphati-dylcholine; PD, Parkinson's disease; PE, phosphatidylethanolamine; PG, phosphatidylglycerol; PI, phosphatidylinositol; PS, phosphatidylserine; R_f, retention factor; SM, sphingomyelin; TLC, thin-layer chromatography.

Simona Lobasso and Paola Tanzarella contributed equally to the work.

1 | INTRODUCTION

Parkinson's disease (PD) is considered a complex disease with a multifactorial etiology, where a combination of genetic and environ- mental factors are thought to contribute in the majority of cases (Kitada, Tomlinson, Ao, Grimes, & Schlossmacher, 2012; Klein & Schlossmacher, 2006). Three main molecular defects are associated with neurodegeneration and PD pathogenesis: (1) accumulation of misfolded and aggregated proteins; (2) impairment of cellular processes such as the autophagy–lysosomal pathway and ubiquitin– proteasome system; (3) oxidative stress together with mitochondrial dysfunction (Burke, 2004; Cookson, 2012; Dawson & Dawson, 2003; Valente, Arena, Torosantucci, & Gelmetti, 2012).

Only rare PD cases are due to a single genetic cause (Klein & Schlossmacher, 2006), among these are autosomal recessive muta- tions in *parkin* (PARK-2) gene, which are correlated with early-onset familial form of PD (Cookson, 2012; Dodson & Guo, 2007; Xiong et al., 2009). PARK-2 gene encodes parkin, a protein that belongs to the ring between ring (RBR) fingers class of E3 ubiquitin ligases (Kitada et al., 1998; Shimura et al., 2000). It is reported that the absence of the ubiquitin ligase activity in the *parkin*-mutant cells impairs degradation of specific substrates by the ubiquitin–proteasome system, with accumulation of non-ubiquitinated toxic products leading to neuro- degeneration (Dawson, 2006; Sandebring & Cedazo-Minguez, 2012). Parkin is also able to protect mitochondrial function and genomic integrity from oxidative stress (Rothfuss et al., 2009) and to influence fatty acid uptake and metabolism (Abumrad & Moore, 2011; Kim et al., 2011). Furthermore, a recent genome-wide RNAi screen performed in PD cell models has found a link between the master regulator of lipid synthesis SREBF1 and PARK-2-mediated mitophagy, underscoring the impact of lipid alteration on PD pathogenesis (Ivatt et al., 2014). Although the parkin protein is localized mainly in cytoplasm, it is present in membranes including lipid rafts too (Fallon et al., 2002; Kubo et al., 2001; Shimura et al., 1999).

Lipid rafts are highly specialized membrane microdomains containing a given set of proteins involved in signal transduction, trafficking of proteins and endo/exocytosis, which are enriched in specific lipids, such as glycosphingolipids and cholesterol (Simons & Toomre, 2000). Recently it has been demonstrated that the loss of parkin causes alterations in lipid-rafts and accumulation of caveolin-1, one of the most important protein involved in lipid-rafts-dependentendocytosis (Cha et al., 2015).

Parkin is expressed in human skin fibroblasts (Hoepken et al., 2007; Mortiboys et al., 2008), whose primary cultures can be easily obtained from skin biopsies of PD patients. Although whole protein pattern, cell signaling and embryonic origin of skin fibroblasts differ from neurons, many reports have showed that *parkin*-mutant fibroblast cultures mirror the protein expression, the mitochondrial respiratory alterations and the vulnerability to proteasomal stress of other neuronal model systems (Auburger et al., 2012; Del Hoyo et al., 2010; Grünewald et al., 2010).

Previous studies have shown that primary fibroblasts of two different Italian *parkin*-mutant patients, affected by early-onset autosomal recessive PD, both resulting in the absence of the full length protein, displayed severe ultrastructural abnormalities, mainly in mitochondria, impaired energy metabolism and increased reactive oxygen species (ROS) production (Ferretta et al., 2014; Pacelli et al., 2011; Vergara et al., 2014). In addition, modifications of the expression level of several proteins involved in cytoskeleton structure dynamics, calcium homeostasis, oxidative stress response protein, and RNA processing have been found in the cells (Lippolis et al., 2015).

In the present study, we have extended the biochemical characterization of these *parkin*-mutant fibroblasts by studying their lipid profiles by coupled TLC and MALDI-TOF mass spectrometry (MS) analyses. In parallel, direct MALDI-TOF/MS lipid analyses of intact *parkin*-mutant fibroblasts have been performed by skipping lipid extraction steps.

Thanks to the two different analytical approaches, the results indicate that increased levels of specific glycosphingolipid species (the GM2 and GM3 gangliosides) as well as of phospholipids lysophos- phatidylcholine, phosphatidylserine, and phosphatidylinositol are present in parkin lacking fibroblasts. Advantages and caveats of thetwo different analytical approaches in lipid profiling of fibroblasts are briefly discussed.

2 | MATERIALS AND METHODS

2.1 | Materials

All organic solvents used were commercially distilled and of the highest available purity (Sigma–Aldrich). The matrix used for MALDI- TOF/MS analyses was the 9-aminoacridine hemihydrate (9-AA) and was purchased from Acros Organics. 1,1′,2,2′-tetratetradecanoyl cardiolipin, 1,1′2,2′-tetra-(9Z-octadecenoyl) cardiolipin, 1,2-ditetra- decanoyl-*sn*-glycero-3-phosphate, 1,2-ditetradecanoyl-*sn*-glycero-3- phospho-(1′-rac-glycerol), 1,2-ditetradecanoyl-*sn*-glycero-3-phos- pho-L-serine, 1,2-di-(9Z-hexadecenoyl)-*sn*-glycero-3-phosphoethanolamine were purchased from Avanti Polar Lipids, Inch. Plates for TLC (Silica gel 60A, 10 × 20 cm, 0.2 mm thick layer), obtained from Merck (Darmstadt, Germany), were washed twice with chloroform/methanol (1:1, v/v) and activated at 120 °C before use.

2.2 | Primary fibroblasts and culture conditions

Primary skin fibroblasts were obtained from two unrelated patients affected by an early-onset PD, with *parkin* compound heterozygous mutations, named *parkin*-mutant1 with del exon7-9/Glu409X (Ferretta et al., 2014; Lippolis et al., 2015) and *parkin*-mutant2 with del exon2-3/del exon3 (Lippolis et al., 2015; Pacelli et al., 2011; Vergara et al., 2014), and from a healthy subject, named control1 (Ferretta et al., 2014; Lippolis et al., 2015; Pacelli et al., 2011; Vergara et al., 2014), by explants from skin punch biopsy, after informed consent. The biopsies were taken in parallel and processed simultaneously to establish primary cell lines. Adult normal human dermal fibroblasts (NHDF), purchased from Lonza Walkersville Inc. (Walkersville, MD), were also utilized, named control2.

Cells were grown in high-glucose Dulbecco's modified Eagle's medium (DMEM) supplemented with 10% (v/v) fetal bovine serum (FBS), 1% (v/v) L-glutamine, 1% (v/v) penicillin/streptomycin, at 37 °C in a humidified atmosphere of 5% CO_2. All experiments were performed on cells with equal passage numbers, ranging from 5 to 14, to avoid an artifact due to senescence, known to occur at passage numbers greater than 30. In the passage range used, fibroblasts were β-Gal negative (Dimri et al., 1995). For the experimental conditions, the media were removed and the cells were washed with phosphate- buffered saline (PBS); then, the cells were incubated with trypsin for 2 or 3 min, harvested by centrifugation at 500*g* for 3 min and finally suspended in distilled water.

2.3 | Lipid extraction

Total lipids of the PD skin fibroblast preparations and of the controls were extracted by the Bligh and Dyer method (Bligh & Dyer, 1959); the extracts were carefully dried under N_2 before weighing and then dissolved in chloroform (10 mg/ml). The lipid/protein ratio was about 0.2 (w/w) in the cell lines here considered. Lipid extracts of three different *parkin*-mutant1 fibroblast cultures and of three different control1 fibroblast cultures were analyzed in the present study.

2.4 | Thin-layer chromatography (TLC)

Total lipid extracts were analyzed by TLC on silica gel plates and lipids were eluted with either Solvent A, chloroform/methanol/acetic acid/ water (85:15:10:3.5, v/v) or Solvent B, chloroform/methanol/water/ ammonium hydroxide 25% (120:75:6:2, v/v).

Total lipids were detected by spraying TLC plates with 5% sulfuric acid, followed by charring at 120 °C or alternatively with a solution of primuline (Fuchs, Schiller, Süss, Schürenberg, & Suckau, 2007) and visualized upon excitation by UV light (336 nm). In addition, molybdenum blue reagent (Sigma–Aldrich) was used as staining specific for phospholipids. Individual phospholipids were identified by reference to authentic lipid standards (Avanti Polar Lipids). Quantita- tive analysis of the lipid spots from the TLC plate was performed by video densitometry, using the software ImageJ. In order to analyze in detail the various components of the lipid extracts, bands present on plates were scraped and lipids extracted from silica, as previously described (Kates, 1986); briefly, 30 µl of a mixture chloroform/ methanol (1:1, v/v) have been added to silica bands, then the samples were vigorously stirred and then centrifuged. Lipid bands were then analyzed by positive and negative ion modes MS.

2.5. MALDI-TOF/MS

MALDI-TOF mass spectra were generally acquired in the negative and positive modes on a Bruker Microflex LRF mass spectrometer (Bruker Daltonics, Bremen, Germany). The system utilizes a pulsed nitrogen laser, emitting at 337 nm, the extraction voltage was 20 kV, and gated matrix suppression was applied to prevent detector saturation. For each mass spectrum, 2000 single laser shots (sum of 4 × 500) were averaged. The laser fluence was kept about 5% above threshold to have a good signal-to-noise ratio. All spectra were acquired in reflector mode (detection range: 500–2000 mass/charge, *m*/*z*) using the delayed pulsed extraction; spectra were acquired in negative and positive modes. A mix containing 1,1′,2,2′-tetratetradecanoyl cardiolipin, 1,1′,2,2′-tetra-(9Z-octadecenoyl) cardiolipin, 1,2-ditetradeca- noyl-*sn*-glycero-3-phosphate, 1,2-ditetradecanoyl-*sn*-glycero-3- phospho-(1′-rac-glycerol), 1,2-ditetradecanoyl-*sn*-glycero-3-phos- pho-L-serine, and 1,2-di-(9Z-hexadecenoyl)-*sn*-glycero-3-phosphoethanolamine, was always spotted next to the sample as external standard and an external calibration was performed before each measurement; the mass range of the authentic standards is 590–1460 atomic mass units (amu). For MS/MS analyses, a Bruker Daltonics Ultraflex Extreme MALDI/TOF TOF mass spectrometer has been used (Bruker Daltonics).

Samples for MALDI-TOF analysis were prepared as previously described (Sun et al., 2008). Briefly, the total lipid extracts (10 mg/ml) were diluted from 20 to 200 μl with a 60:40 (v/v) 2-propanol/ acetonitrile mixture. Next, 10 µl of a diluted sample was mixed with 10 µl of 9-AA (20 mg/ml) dissolved in a 60:40 (v/v) 2-propanol/ acetonitrile mixture. Then 0.35 µl of the mixture was spotted on the MALDI target (Micro Scout Plate, MSP 96 ground steel target). When indicated, lipids from intact fibroblasts were directly analyzed by "intact method," as previously described (Angelini et al., 2012).

Peaks areas, spectral mass resolutions, and signal-to-noise ratios were determined by the software for the instrument *Flex Analysis 3.3* (Bruker Daltonics). A specific lipid database (Lipid Maps Database, http://www.lipidmaps.org) was used to facilitate and confirm the assignment of

lipid species.

In our study, mass spectra of three independent biological samples (i.e., three cell cultures and the corresponding lipid extracts) were considered to confirm reproducibility of the results. In particular, series of MALDI mass spectra (three replicates for each sample) have been averaged by using the software for the instrument *ClinProTools 3.0* (Bruker Daltonics) in order to gain peaks showing significant differ- ences in intensities between different series of spectra (control and *parkin*-mutants). A *p*-value from paired Student's *t*-test <0.05 was set as the threshold to define significant differences between the two series of spectra.

3 | RESULTS

In the present study, we have analyzed the lipid extracts of *parkin*- mutant fibroblasts by coupled TLC and MALDI-TOF/MS techniques. In parallel, direct MALDI-TOF/MS lipid analyses of intact fibroblastshave been performed by skipping lipid extraction steps.

3.1 | Analyses of the lipid extracts of control and *parkin*-mutant1 fibroblasts

Figure 1a shows the comparison between the representative lipid profiles of *parkin*-mutant1 and control1 fibroblasts obtained by negative ion MALDI-TOF/MS analysis of the lipid extracts. The two lipid patterns are dominated by signals in the *m*/*z* range 700–900 compatible with major glycerophospholipid species; minor signals are present in the *m*/*z* range 1000–1500 attributable to glycosphingoli- pids and cardiolipin (CL). In the range of major phospholipids, the small peaks at *m*/*z* 747.5 and 766.5 are attributable to phosphatidylglycerol (PG) 34:1 and phosphatidylethanolamine (PE) 38:4, respectively, while the one at *m*/*z* 788.5 to phosphatidylserine (PS) 36:1. Various species of phosphatidylinositol (PI) are present in both the mass spectra at *m*/*z*835.6 (PI 34:1), *m*/*z* 861.5 (PI 36:2), *m*/*z* 885.5 (PI 38:4), and *m*/*z* 909.5 (PI 40:6). Furthermore, the small peak at *m*/*z* 1452.1 (highlighted by asterisk in the inset), visible in the lipid profiles in the enlargement of Figure 1a, corresponds to the phospholipid CL 72:6, the most abundant CL species in human skin fibroblasts (El-Hafidi et al., 2011). The identification of the MALDI signal at *m*/*z* 1452.1 was confirmed by MS/MS analysis (not shown).

The small peaks at *m*/*z* 1151.7, 1263.8, and 1466.9 present in the (−) MALDI-TOF/MS lipid profile of *parkin*-mutant1 fibroblasts are almost undetectable in control1 fibroblasts (Figure 1a). Additional peaks at *m*/*z* 1235.8, 1354.8, and 1438.9, whose intensity is higher in the lipid profile of *parkin*-mutant1 fibroblasts than in that of control ones, can be observed in the *m*/*z* 1000–1600 enlargement of the mass spectra (Figure 1a, inset). Most of these MALDI signals are compatible with acidic glycosphingolipids, carrying three or four sugar residues in their molecules, named GM3 and GM2. Interestingly, these glycosphingolipids can be detected by negative ion MALDI-TOF mass spectrometry although they are minor components in the total lipid extract of fibroblasts (see pale ganglioside spots in TLC of Figure 2). The chemical identities of MALDI/TOF signals at *m*/*z* 1466.9 and *m*/*z* 1263.8 have been defined by MS/MS analysis and are assigned to gangliosides GM2 24:0 and GM3 24:0, respectively (Supplementary Figure S1). The main signals in the MALDI-TOF mass spectra, attributable to the negative $[M-H]^-$ molecular ions of phospholipidsand sphingolipids, are collected in Table 1.

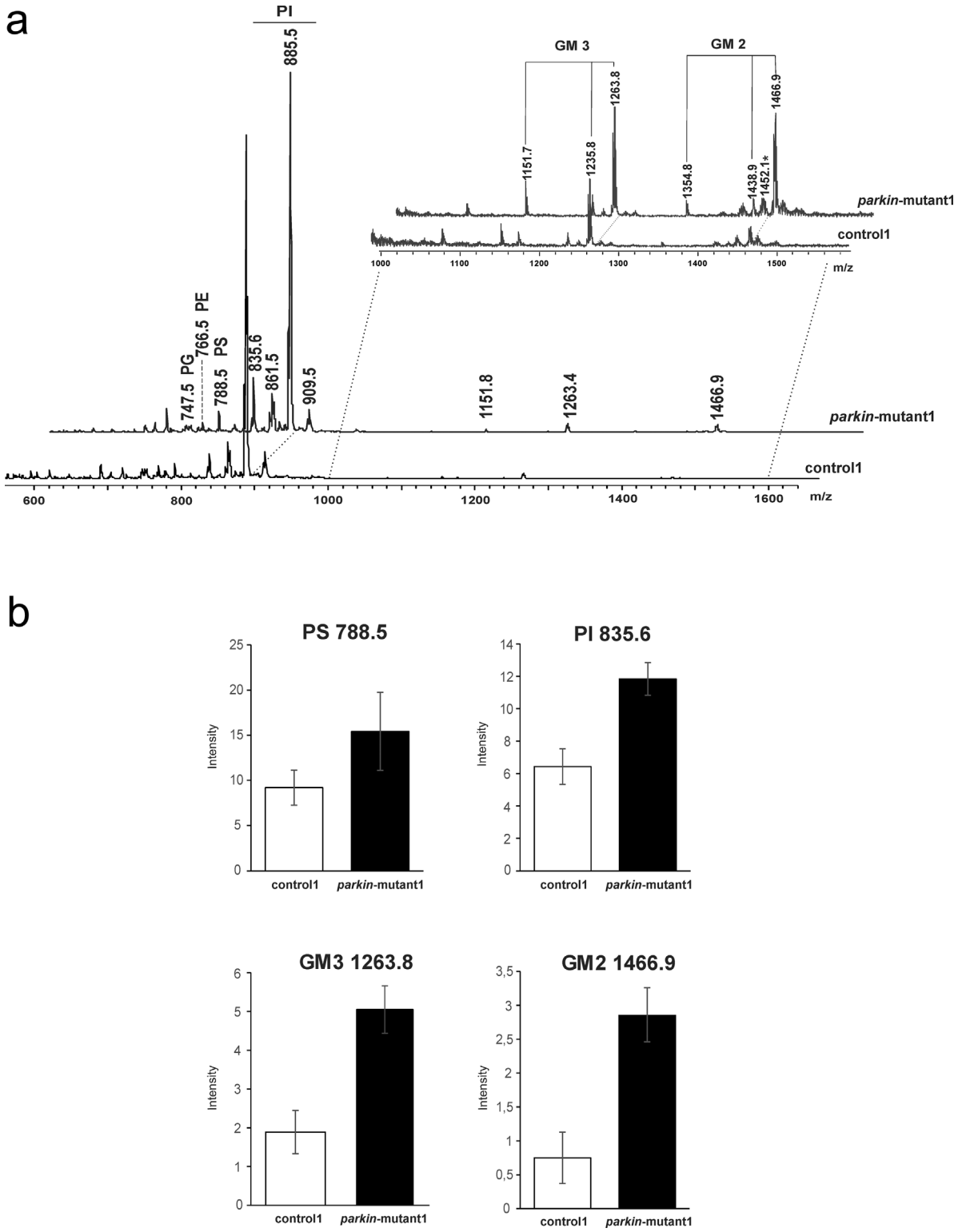

FIGURE 1 Negative ion mode MALDI-TOF/MS analyses of the lipid extracts of fibroblasts of the patient (*parkin*-mutant1) and the healthy control (control1). In (a) two typical lipid profiles are shown. One species for each lipid classes is reported: PG 34:1 $[M-H]^-$ at *m*/*z* 747.5; PE 38:4 $[M-H]^-$ at *m*/*z* 766.5; PS 36:1 $[M-H]^-$ at *m*/*z* 788.5; PI 38:4 $[M-H]^-$ at *m*/*z* 885.5. In the inset, the close-up in the range of *m*/*z* 1000–1600 shows the peaks at *m*/*z* 1151.7, 1235.8, and 1263.8 attributed to gangliosides GM3 and those at *m*/*z* 1354.8, 1238.9, and 1466.9 attributed to GM2. The small peak at *m*/*z* 1452.1 (highlighted by asterisk) corresponds to CL 72:6. In (b) histograms show the significant differences in intensity of lipid peaks at *m*/*z* 788.5, 835.6, 1263.8, and 1466.9. Data are reported as the average value ± SD

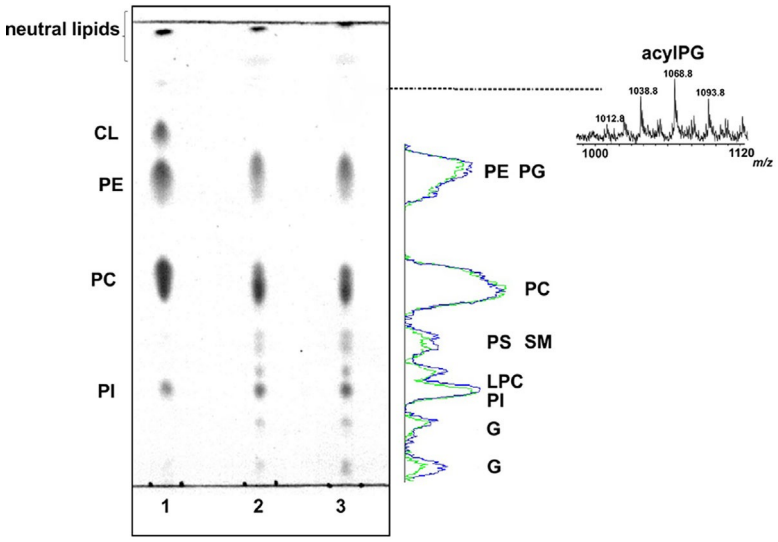

FIGURE 2 Comparison of TLC lipid profiles of *parkin*-mutant1 and control1 fibroblasts. Lipids were eluted with Solvent A and detected by spraying with 5% sulfuric acid and charring at 120 °C. Densitometric evaluation of TLC profiles (2, blue line and 3, green line) has been reported. Lipid bands are indicated by their abbreviations. Thirty micrograms of the total lipid extracts of rat liver mitochondria (1), of control1 (2), and *parkin*-mutant1 fibroblasts (3) were loaded on the plate. On the right of TLC, the negative ion mass spectrum obtained by MALDI scanning of the lane indicated by the dashed line covered with matrix is shown; the higher *m*/*z* peaks present in the spectrum are attributable to acylPG (or Hemi BMP) species

By comparing series of replicates of *parkin*-mutant1 and control1 mass spectra, we found that the following peaks were significantly higher in patient sample: PI 34:1 at *m*/*z* 835.6 and PS 36:1 at *m*/*z* 788.5 plus the gangliosides GM2 24:0 and GM3 24:0 (at *m*/*z* 1466.9 and *m*/*z* 1263.8, respectively) (see Figure 1b).

To gain further information on the lipid composition of *parkin*- mutant1 fibroblasts, the lipid extracts of *parkin*-mutant1 and control1 fibroblasts were analyzed by TLC (Figure 2). The use of an acid eluent allows the separation of polar lipids, while neutral lipids run close to the solvent front. Individual polar lipids were identified by comparison of

TABLE 1 Assignments of *m/z* values detected in the negative ion mode MALDI-TOF mass spectra of lipids from fibroblasts

m/z Value	Assignment $[M-H]^-$	*m/z* Value	Assignment $[M-H]^-$
645.4	PA 32:1	913.6	PI 40:4
673.5	PA 34:1	1012.8	18:1–18:1–16:0 Hemi BMP
701.6	SM 16:0	1038.8	18:1–18:1–18:1 Hemi BMP
717.4	PG 32:2	1068.8	18:1–20:0–18:1 Hemi BMP
726.5	PE (O-18:1/18:1)	1093.8	20:0–20:0–18:1 Hemi BMP
744.5	PE 36:1	1151.7	GM3 16:0
747.5	PG 34:1	1235.8	GM3 22:0
766.5	PE 38:4	1263.8	GM3 24:0
773.5	PG 36:2	1354.8	GM2 16:0
788.5	PS 36:1	1425.9	CL 70:5
810.5	PS 38:4	1438.9	GM2 22:0
835.6	PI 34:1	1452.1	CL 72:6
861.5	PI 36:2	1466.9	GM2 24:0
863.5	PI 36:1	1475.9	CL 72:6 (+Na)
883.6	PI 38:5	1601.9	GM1 22:0
885.5	PI 38:4	1698.9	GM1 18:0
909.5	PI 40:6	1795.9	GM1 18:0
911.6	PI 40:5		

The numbers (x:y) denote the total length and number of double bounds of both acyl chains, except for PE (O-18:1/18:1) in which the acyl chain in *sn*-1 position is replaced with an alkenyl. For SM species, the numbers correspond to the length and number of double bounds of the acyl chain, attached to the sphingosine base. For CL species, the number refers to the two pairs of acyl chains.
CL, cardiolipin; PA, phosphatidic acid; PE, phosphatidylethanolamine; PS, phosphatidylserine; PG, phosphatidylglycerol; PI, phosphatidylinositol; SM, sphingomyelin; GM1, GM2, GM3, gangliosides; Hemi BMP, Hemi Bis(Monoacylglycero)Phosphate (or AcylPG).

their retention factor (R_f) values with those of lipid standards and by their response to specific lipid staining (not shown). The polar lipids of fibroblasts were identified (in R_f order) as gangliosides (G), phosphatidylinositol, lysophosphatidylcholine (LPC), phosphatidylserine, sphingomyelin (SM), phosphatidylcholine (PC), phosphatidylglycerol, phosphatidylethanolamine. It can be observed that PC is the most abundant phospholipid in the plasma membrane of fibroblasts; CL, the lipid marker of mitochondria, was not detectable in this analysis. The same lipid bands are present in the TLC profiles of the two different lipid extracts; individual bands of each lipid extract have been isolated and MALDI-TOF analyses (either in the negative or positive mode) of the lipids extracted from silica confirmed above assignments (not shown). By performing densitometric analyses of lipid bands, it can be noted that the intensities of lipid spots of G, PI, and PS are higher in *parkin*-mutant1 than in control1 fibroblasts, according to MALDI-TOF/MS results (Figure 1).

In order to check for minor classes of lipids, we have also scraped silica corresponding to lipid bands barely stained, and extracted lipids. Interestingly, the MALDI-TOF spectrum of lipids isolated from a TLC area having R_f 0.77 (close to the solvent front) has revealed the presence of hemi bis (monoacylglycero) phosphate (Hemi BMP) (see Figure 2, inset). Hemi BMPs (i.e., acylPG) contain a glycerophospho- glycerol backbone with three fatty acyl chains esterified to the glycerol hydroxyls; in particular, the peaks at *m/z* 1012.8, *m/z* 1038.8, *m/z* 1068.8, and *m/z* 1093.8 are identified as 18:1–18:1–16:0 Hemi BMP, 18:1–18:1–18:1 Hemi BMP, 18:1–18:1–20:4 Hemi BMP, and 20:4–20:4–18:1 Hemi BMP, respectively.

In addition, the lipid extracts of *parkin*-mutant1 and control1 fibroblasts were comparatively analyzed by using a basic eluent in TLC analyses. Lipid bands were assigned to different lipid species by comparison with authentic standards (see Supplementary Figure S2). The main difference in the two lipid profiles was in the band of lowest R_f having a much higher intensity in *parkin*-mutant than in control. Figure 3 shows the lower part of the TLC plate: it can be seen that both control1 and *parkin*-mutant1 upper bands (R_f 0.17) contain SM species (see corresponding positive ion mode mass spectra in the upper panels). The lower lipid spot (R_f 0.07), present in the *parkin*-mutant1 profile, contained the peaks at *m/z* 496.3 and *m/ z* 522.3 assigned to two species of LPC 16:0 and LPC 18:1, respectively (see positive ion mode MALDI mass spectra in the lowerpanels of Figure 3).

These two LPC species can be also observed in the positive ion MALDI-TOF/MS lipid profile of *parkin*-mutant 1 fibroblasts (see Supplementary Figure S3 and Figure 5 in the following). The main signals in the MALDI-TOF mass spectra, attributable to the positive $[M+H]^+$ molecular ions of phospholipids and neutral glycosphingolipidsare collected in Table 2.

In summary, in the lipid extract of *parkin*-mutant1 fibroblasts we found higher levels of two glycosphingolipids, the anionic gangliosides GM2

and GM3, and of phospholipids PI, LPC, and PS.

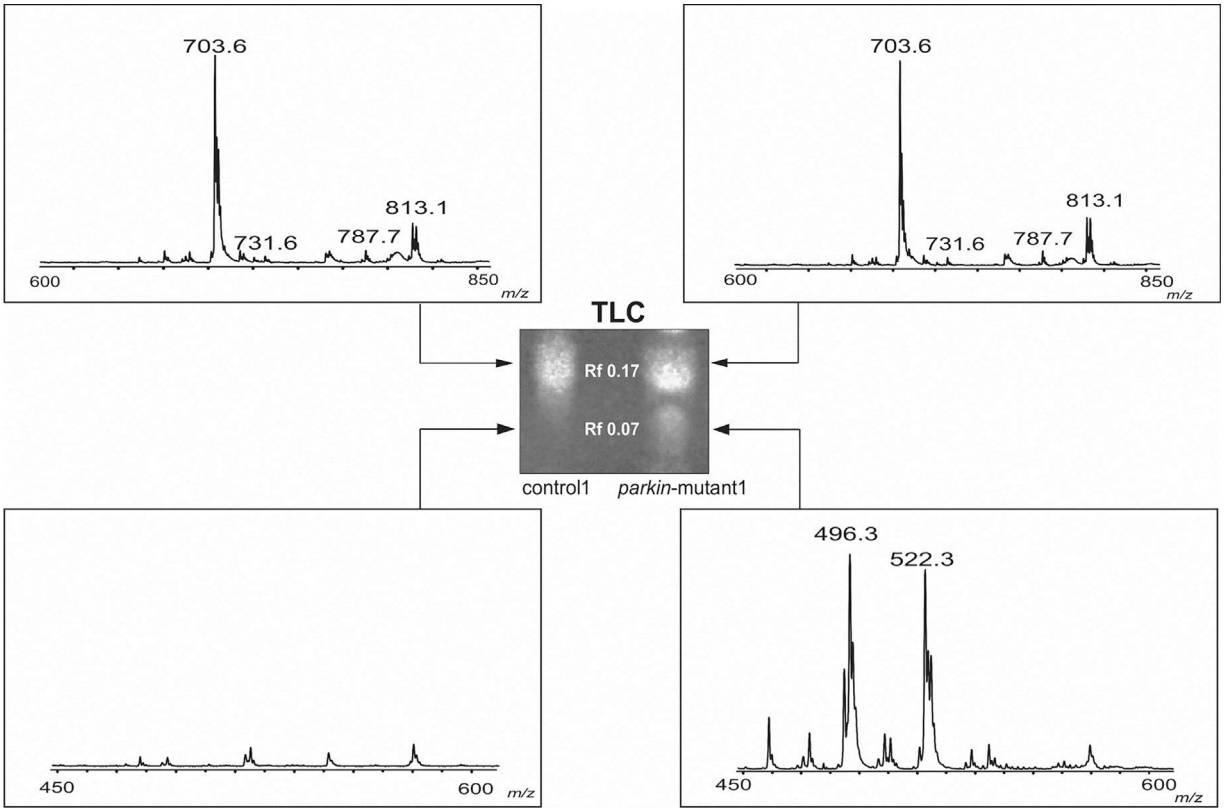

FIGURE 3 LPC enrichment in *parkin*-mutant1 fibroblasts detected by coupled MALDI-TOF/MS and TLC. Lipids were eluted with Solvent B and detected with primuline. The whole chromatogram is shown in Supplementary Figure S2, while here the lower part of the same TLC is reported. Sixty micrograms of the total lipid extracts of control1 and *parkin*-mutant1 fibroblasts were loaded on the plate. In the upper panels, the positive ion MALDI-TOF mass spectra of the lipid bands having R_f 0.17 are shown, while in the lower panels those of the lipid bands having R_f 0.07 are shown. The two peaks at *m*/z 496.3 and *m*/z 522.3 have been assigned to LPC 16:0 and LPC 18:1, respectively

TABLE 2 Assignments of *m/z* values detected in the positive ion mode MALDI-TOF mass spectra of lipids from fibroblasts

m/z Value	Assignment $[M+H]^+$	*m/z* Value	Assignment $[M+H]^+$
496.3	LPC 16:0	810.6	PC 38:4
522.3	LPC 18:1	813.1	SM 24:1
703.6	SM 16:0	1466.9	NG
731.6	SM 18:0	1494.9	NG
732.5	PC 32:1	1519.8	NG
760.6	PC 34:1	1546.8	NG
786.6	PC 36:2	1568.9	NG
787.7	SM 22:0	1603.9	NG

The numbers (x:y) denote the total length and number of double bounds of both acyl chains. For LPC species, the number corresponds to the length and number of double bounds of the only acyl chain. For SM species, the numbers correspond to the length and number of double bounds of the acyl chain, attached to the sphingosine base.
SM, sphingomyelin; LPC, lysophosphatidylcholine; PC phosphatidylcholine; NG, neutral glycosphingolipids.

3.2 | Direct analyses of intact fibroblasts byMALDI-TOF/MS

Recently MALDI-TOF/MS analysis has been successfully used to directly acquire lipid profiles of biological samples (Angelini, Babudri, Lobasso, & Corcelli, 2010; Angelini et al., 2012, 2015; Angelini, Vortmeier, Corcelli, & Fuchs, 2014; Vitale et al., 2015). One of the advantages of this analytical approach is that minute amounts of cell membranes are required for lipid analyses. On these bases, we have also performed direct MALDI-TOF/MS lipid analysis of intact fibroblasts; besides the *parkin*-mutant1 sample, primary fibroblasts obtained from another unrelated patient, affected by an early-onset PD, having a different *parkin*-null mutation and here named *parkin*- mutant2 (Vergara et al., 2014), have been also analyzed. In order to match the number of control samples with that of patients, we also analyzed lipids of the commercial NHDF fibroblast cells (named control2).

Although not perfectly overlapping, the lipid profiles of the two different *parkin*-mutants shared similarities in the comparison with the two controls (Figure 4a). In agreement with above results, the peaks of PI 34:1 (*m/z* 835.6), GM2 24:0 and GM3 24:0 (*m/z* 1466.9 and *m/z* 1263.8, respectively) were significantly higher in both patient samples (see Figure 4b). An additional ganglioside species GM3 16:0 at *m/z* 1151.7 was higher in both patient fibroblasts than in controls (not shown). However, no difference in PS content between the lipid profiles emerged from this analysis; the discrepancy between results of analyses of the lipid extracts and direct lipid membrane analyses could depend on the less sensitivity of the latter experimental approach in the PS detection. On the other hand, the direct analyses of lipids by MALDI-TOF/MS allows the detection of gangliosides with higher sensitivity.

The positive ion mode MALDI-TOF/MS lipid profiles of intact fibroblasts obtained from the two controls, *parkin*-mutant1 and *parkin*- mutant2 patients are shown in Figure 5a. The signals at *m/z* 732.5, *m/z* 760.6, *m/z* 786.6, and *m/z* 810.6 assigned to the molecular ions $[M+H]^+$ of PC species, 32:1, 34:1, 36:2, and 38:4, respectively, are predominant in all the lipid profiles. A small peak at *m/z* 703.6, present in all the lipid profiles, corresponds to the phospholipid SM 16:0. In the *m/z* range between 1400 and 1700 low peaks are attributable to neutral glycosphingolipids, having five or six hexose residues in their structure (Figure 5a, right inset), according to MALDI-TOF mass spectra of total lipid extracts (see Supplementary Figure S3).

In addition, two small peaks at *m/z* 496.3 and *m/z* 522.3, better visible in the two patient samples, correspond to the molecular ions $[M+H]^+$ of LPC 16:0 and 18:1, respectively (Figure 5a, left inset). The comparison of different series of spectra (controls and *parkin*-mutant patients) revealed that the peak at *m/z* 496.3 was significantly higher both in *parkin*-mutant1 and *parkin*-mutant2 patients, while the peak at *m/z* 522.3 was significantly higher in *parkin*-mutant1 only. No significant difference in the PC 34:1 (at *m/z* 760.6) and SM 16:0 (at *m/z* 703.5) content between PDs and controls was found (Figure 5b). In summary, lipid data obtained performing the analyses on intact membranes indicate an increase of gangliosides GM2 and GM3, PI and LPC in the two different *parkin*-mutant samples. Thus, with exception of PS, results obtained by direct MS analysis of intact fibroblasts of*parkin*-mutant1 are in large agreement with the previous analyses performed on mass spectra of their lipid extracts.

4 | DISCUSSION

Deregulated lipid metabolism is increasingly recognized as involved in a growing number of neurodegenerative disorders (Grimm, Tschäpe, Grimm, Zinser, & Hartmann, 2006; Hartmann, Kuchenbecker, & Grimm, 2007). During neurodegeneration and aging, physical and chemical properties of biological membranes can be altered due to lipid oxidation and changes in lipid relative proportions (Grimm et al., 2006;

Hartmann et al., 2007). Surprisingly, only a few studies have previously examined the lipid pathway alterations in brains of PD patients (see for example Cheng et al., 2011; Fabelo et al., 2011; Gegget al., 2015).

The present paper describes the results of an explorative study on cellular lipids of *parkin*-mutant skin fibroblasts. The aim was to check whether loss of parkin induces alterations in the cellular lipid profile. To the best of our knowledge, the data presented herein represent the first lipidomic analysis of human skin fibroblasts lacking the parkin protein. Altogether, our data reveal important rearrangements in the lipidome of *parkin*-mutant fibroblasts. In absence of the parkin protein,data indicate enrichment of (1) the acidic gangliosides GM2 and GM3;
(2) the phospholipids PI and PS; and (3) the lysophospholipids LPC.

Gangliosides are a subgroup of sialylated glycosphingolipids mostly localized in the cellular membrane of glial and neuronal cells; they were first isolated in high quantity from ganglia (hence named gangliosides), but are present on all cells and tissues throughout the body at relatively low levels. They may be involved in the regulation of several cellular events, such as neurotrophy and neurotransmission by physiologically interacting with regulatory proteins (Yu, Nakatani, &Yanagisawa, 2008).

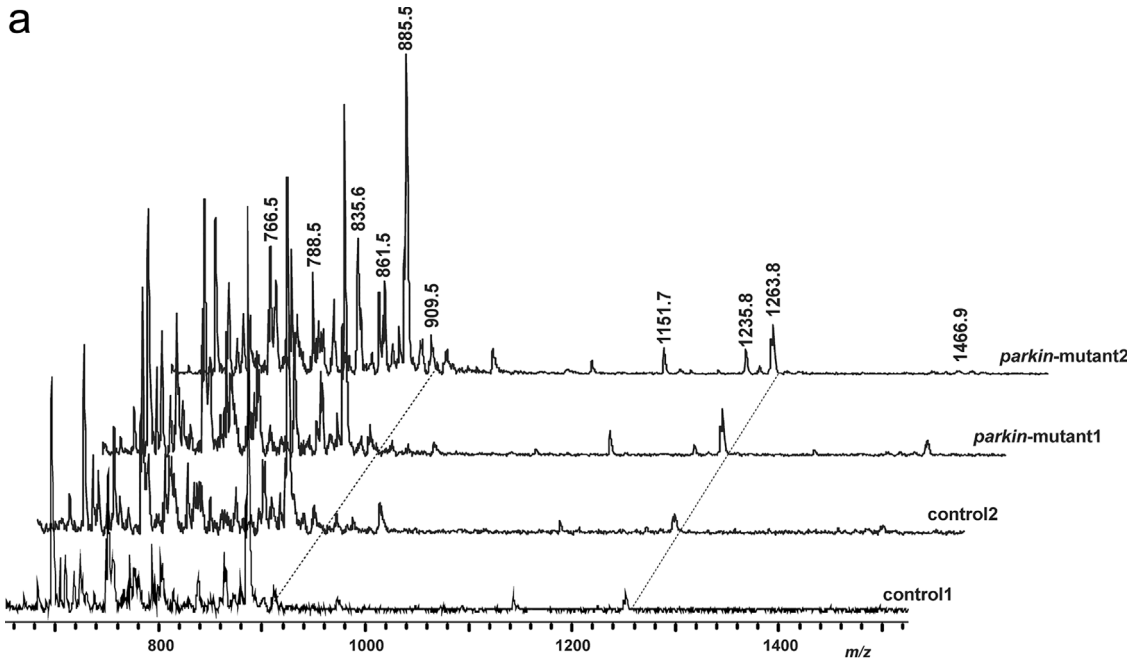

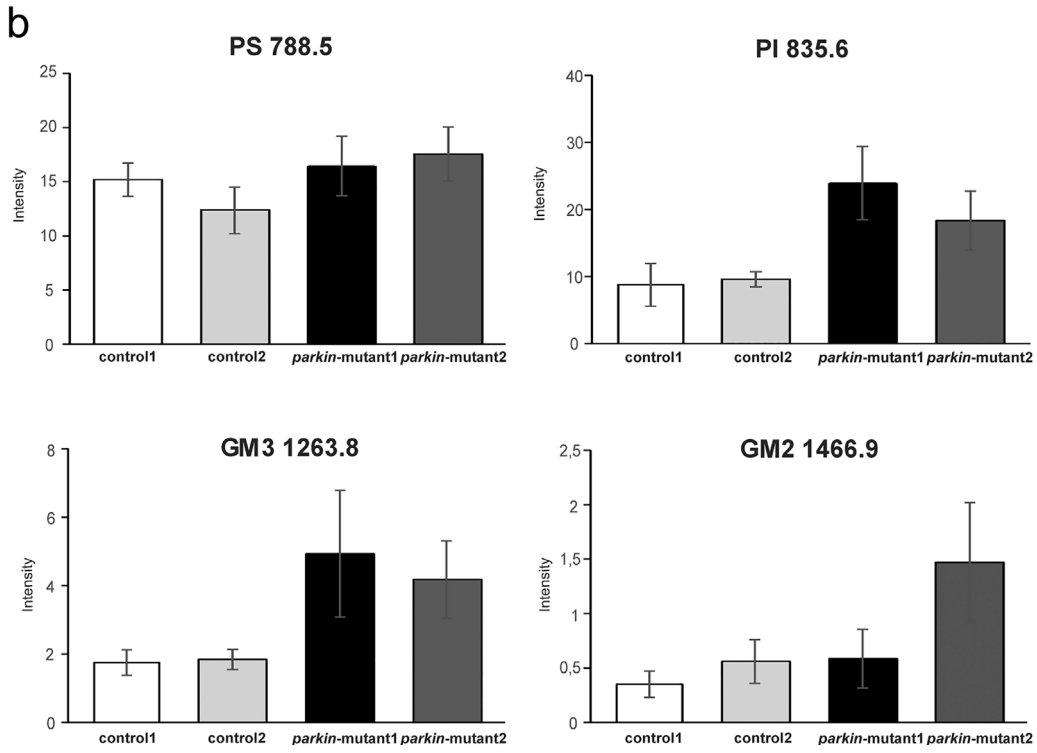

FIGURE 4 Negative ion mode MALDI-TOF/MS lipid profiles of intact fibroblasts of controls (control1 and control2) and patients(*parkin*-mutant1 and *parkin*-mutant2). In (a) mass spectra were acquired directly on intact fibroblast membranes and are representative of three different cultures. In (b) histograms show the differences in intensities of lipid peaks at *m*/*z* 788.5, 835.6, 1263.8, and 1466.9, assigned to PS 36:1, PI 34:1, GM3 24:0, and GM2 24:0, respectively. Data are reported as the average value ± SD

It is well known that sphingolipids metabolism is deeply altered in many neurodegenerative diseases and that abnormal sphingolipids patterns are related to their pathogenesis (Piccinini et al., 2010). Gangliosides are involved also in other pathologies, such as GM3 synthase deficiency (Simpson et al., 2004), Tay–Sachs disease (Mahyran, 1999), Sandhoff disease (Martin et al., 2005), and Gaucher's disease (GD) (Fuller, 2010). In particular, patients with GD type 1 share several of the neuropathological features of PD (Sidransky & Lopez, 2012). Thus, nowadays the presence of mutations in the glucocerebrosidase (GBA) gene is considered the most relevant genetic risk factor for developing PD. In fact, some years ago it was found that mutations in the GBA gene when homozygous lead to GD, but when

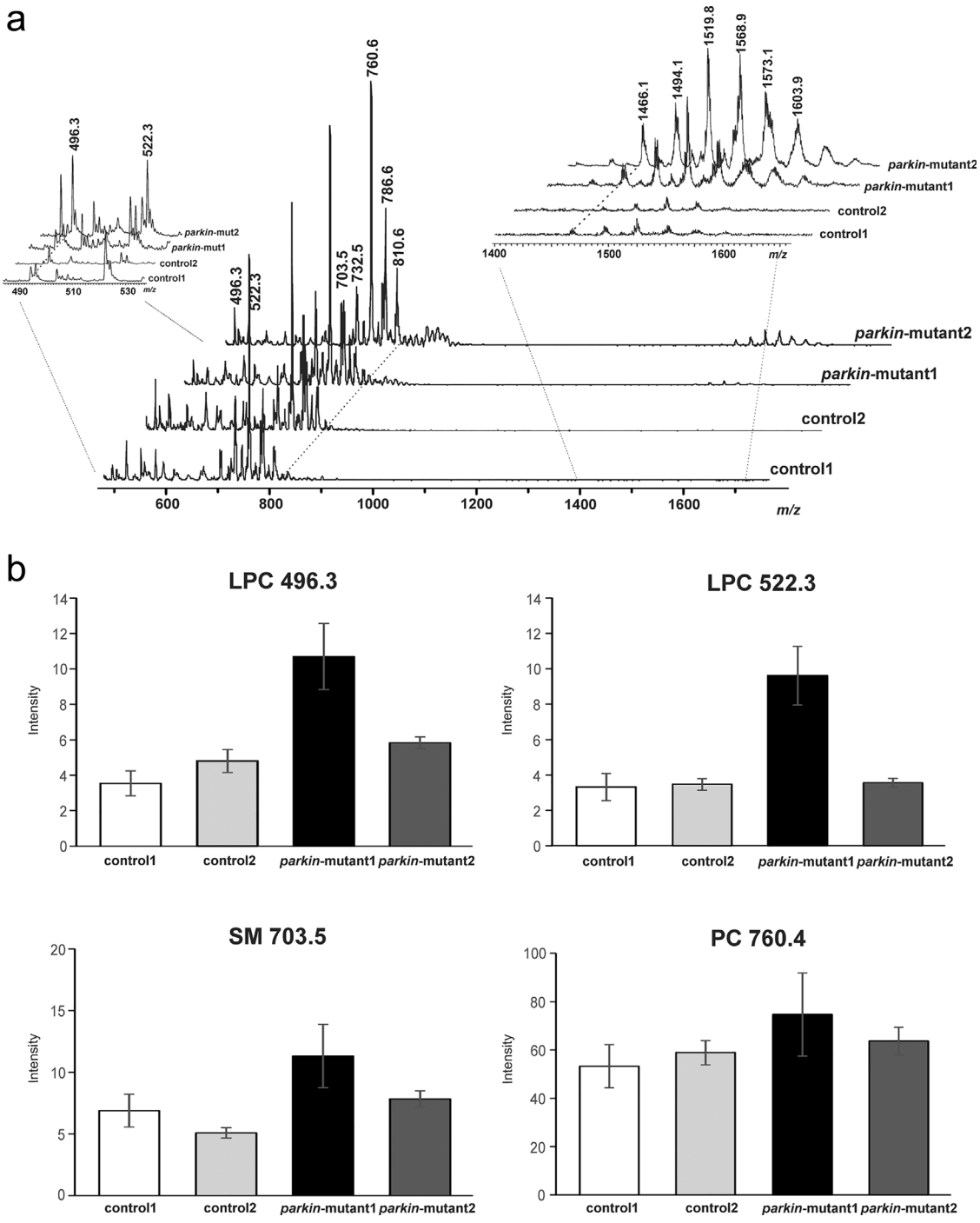

FIGURE 5 Positive ion mode MALDI-TOF/MS lipid profiles of intact fibroblasts of controls (control1 and control2) and patients (*parkin*-mutant1 and *parkin*-mutant2). In (a) mass spectra are acquired directly on intact fibroblast membranes. In the left inset, the close-up in the range of *m*/*z* 485–535 shows peaks attributable to LPC species. In the right inset, the close-up in the range of *m*/*z* 1400–1700 shows peaks attributable to neutral gangliosides. In (b) histograms show the differences in intensities of lipid peaks at *m*/*z* 496.3, 522.3, 703.5, 760.6 assigned to LPC 16:0, LPC 18:1, SM 16:0, PC 34:1, respectively

heterozygous predispose to PD (Lwin, Orvisky, Goker-Alpan, LaMarca, & Sidransky, 2004; Neumann et al., 2009).

As the lysosomal enzyme GBA is required for the cleavage of the glucosylceramide to glucose and ceramide (Beutler & Gelbart, 1992), it has been suggested that the accumulation of this sphingolipid in lysosomal membranes can trigger the onset of PD and other Lewy body disorders (Mata et al., 2008; Sidransky & Lopez, 2012). Recent findings have suggested that GBA mutations are responsible for defects in autophagy in iPSC-derived neurons from patients with GD and PD, thus underlining their vulnerability to neurodegeneration (Schöndorf et al., 2014). On other hand, it was established a link between deregulated sphingolipid metabolism and α-synuclein accumulation (Mazzulli et al., 2011), a lipid-binding protein, linked genetically and neuropathologically to PD (Polymeropoulos et al., 1997), responsible for misfolding events causing neurotoxicity (Gai et al., 2000; Spillantini et al., 1997). A recent study has reported that artificial membrane vesicles composed of gangliosides GM1 and GM3 are able to accelerate the α-synuclein aggregation, suggesting that these exosomes could provide catalytic environment for nucleation of this process involved into PD pathogenesis (Grey et al., 2015). Recently, the molecular interaction of gangliosides with α-synucleinhas been studied in PD human cell lines (Di Scala et al., 2016).

In general, the distribution patterns of gangliosides differs in different tissues. In the brain, the most abundant gangliosides are represented by four sialoglycan structures (one pentasaccharide, two hexasaccharides, and one heptasaccharide, respectively, GM1, GD1a, GD1b, and GT1b) (Jackson et al., 2011). The cultured human skin fibroblasts do not contain detectable amounts of these specific gangliosides, but mainly less complex molecules (Dawson, Matalon, & Dorfman, 1972).

Here we detected significant increased levels of anionic ganglio- sides GM2 and GM3 in the *parkin*-mutant fibroblasts, in agreement with a previous study showing altered plasma sphingolipid metabolism in non-GBA mutant PD patients (Mielke et al., 2013). In parkin-lacking fibroblasts, the perturbation of intracellular mechanisms caused by excess of membrane gangliosides could be involved in autophagy dysfunction. The analysis of ganglioside composition in the brain of the PD patients would be useful to confirm the important role of sphingolipid metabolism in the pathological features of the disease.

It has been reported that parkin promotes clearance of depolarized mitochondria by mitophagy, a selective process involving autophagosomes leading to the subsequent degradation by lysosomes (Jin & Youle, 2012; Youle & Narendra, 2011), and that *parkin*-mutants are defective in promoting mitophagy (Lee, Nagano, Taylor, Lim, & Yao, 2010). Previous studies showed that both the two cell lines of *parkin*- mutant fibroblasts, whose lipid composition has been here character- ized, presented altered mitochondrial morphology together with reduced respiratory chain Complex I activity and ATP production (Ferretta et al., 2014; Pacelli et al., 2011). The impairment of mitochondrial functions in PD leads us to consider the involvement of lipids of mitochondria in the cellular pathological processes. Therefore, we looked for possible differences in CL content and the presence of CL-oxidized products in *parkin*-mutant fibroblasts. The analyses of the lipid extracts did not show significant CL differences between control and mutant fibroblasts. On the other hand, in the mass spectra acquired on intact fibroblast membranes the CL signal was barely distinguishable from the background, indicating that the CL ionization is favored in the lipid solutions. Finally, we could not detectCL oxidized species in our experimental conditions.

The higher level of the phospholipids PI and PS here detected could be linked to dysfunction in mitochondrial turnover and/or in endoplasmic reticulum organization. It is also possible that these modifications (together with higher sphingolipid content) reflect a change in lipid-raft composition, in agreement with a previous study(Fabelo et al., 2011).

We found a higher LPC content in the lipid profile of *parkin*- mutant fibroblasts compared to healthy controls, and in particular of LPC 18:1 and LPC 16:0 species. Previous studies have suggested that the appearance of the PC derivative LPC is correlated with the pathogenesis of several diseases, and the PC/LPC ratio can be utilized to screen the severity of inflammatory states (Angelini et al., 2014). PD, as other neurodegenerative diseases, is also recognized to have an inflammatory component, yet poorly understood (Qin et al., 2007). In agreement with these findings, the lipid analysis of the *substantia nigra* region of an early-stage rat model of PD has revealed the up-regulation of the same LPC species, which are considered crucial for neuroinflammatory signaling (Farmer, Smith,Hayley, & Smith, 2015).

In the present study the lipid analyses have been performed either by classical techniques, such as TLC and MALDI-TOF/MS analysis of the lipid extracts of fibroblasts, or by direct MS analyses of intact fibroblasts, thus skipping the lipid extraction steps (Angelini et al., 2012). We have shown that MALDI-TOF/MS analysis of intact fibroblasts can also represent a fast and reliable analytical approach that requires only minute amounts of samples to profile lipids of *parkin*-mutant cell lines. With few exceptions, the different lipid classes can be detected by direct lipid analyses of cell membranes. As only a small number of Petri dishes of cultured fibroblasts are required to perform the lipid analyses in intact membranes, the method offers the possibility to fast screening a large number of patients. Furthermore, as the intact method is not only valid for cultured cell membranes, but also for tissues, blood, and isolated organelles, it would be interesting to check for the lipid profiles of neuronal tissuefrom *parkin*-mutant animal models, by the same method.

Understanding the nature of changes in the lipid composition in neurodegenerative disorders can be crucial to develop novel therapeutic strategies and to identify lipid biomarkers for the diagnosisand therapeutic monitoring of the disease.

ACKNOWLEDGMENTS

This work was supported by local grants of the University of Bari to

A.C. and by Sanofi-Aventis Deutschland GmbH, 65926 Frankfurt amMain, Germany to T.C.

REFERENCES

Abumrad, N. A., & Moore, D. J. (2011). Parkin reinvents itself to regulate fatty acid metabolism by tagging CD36. *Journal of Clinical Investigation*, *121*(9), 3389–3392.

Angelini, R., Babudri, F., Lobasso, S., & Corcelli, A. (2010). MALDI-TOF/MS analysis of archaebacterial lipids in lyophilized membranes dry-mixed with 9-aminoacridine. *Journal of Lipid Research*, *51*(9), 2818–2825.

Angelini, R., Vitale, R., Patil, V. A., Cocco, T., Ludwig, B., Greenberg, M. L., & Corcelli, A. (2012). Lipidomics of intact mitochondria by MALDI-TOF/ MS. *Journal of Lipid Research*, *53*, 1417–1425.

Angelini, R., Vortmeier, G., Corcelli, A., & Fuchs, B. (2014). A fast method for the determination of the PC/LPC ratio in intact serum by MALDI-TOF MS: An easy-to-follow lipid biomarker of inflammation. *Chemistry and Physics of Lipids*, *183*, 169–175.

Angelini, R., Lobasso, S., Gorgoglione, R., Bowron, A., Steward, C. G., & Corcelli, A. (2015). Cardiolipin fingerprinting of leukocytes by MALDI- TOF/MS as a screening tool for Barth syndrome. *Journal of Lipid Research*, *56*(9), 1787–1794.

Auburger, G., Klinkenberg, M., Drost, J., Marcus, K., Morales-Gordo, B., Kunz, W. S., … Jendrach, M. (2012). Primary skin fibroblasts as a model of Parkinson's disease. *Molecular Neurobiology*, *46*, 20–27.

Beutler, E., & Gelbart, T. (1992). Mutation analysis in Gaucher disease. *American Journal of Medical Genetics*, *44*, 389–390.

Bligh, E. G., & Dyer, W. J. (1959). A rapid method of total lipid extraction andpurification. *Canadian Journal of Biochemistry and Physiology*, *37*,911–917.

Burke, R. E. (2004). Recent advances in research on Parkinson disease: Synuclein and parkin. *The Neurologist*, *10*, 75–81.

Cha, S. H., Choi, Y. R., Heo, C. H., Kang, S. J., Joe, E. H., Jou, I., … Park, S. M. (2015). Loss of parkin promotes lipid rafts-dependent endocytosis through accumulation caveolin-1: Implications for Parkinson's disease. *Molecular Neurodegeneration*, *10*, 63.

Cheng, D., Jenner, A. M., Shui, G., Cheong, W. F., Mitchell, T. W., Nealon, J. R., … Garner, B. (2011). Lipid pathway alterations in Parkinson's disease primary visual cortex. *PloS ONE*, *6*(2), e17299.

Cookson, M. R. (2012). Parkinsonism due to mutations in PINK1, parkin, and DJ-1 and oxidative stress and mitochondrial pathways. *Cold Spring Harbor Perspectives in Medicine*, *2*, a009415.

Dawson, T. M., & Dawson, V. L. (2003). Molecular pathways of neurodegeneration in Parkinson's disease. *Science*, *302*, 819–822.

Dawson, G., Matalon, R., & Dorfman, A. (1972). Glycosphingolipids in cultured human skin fibroblasts. I. Characterization and metabolism in normal fibroblasts. *Journal of Biological Chemistry*, *247*, 5944–5950.

Dawson, T. M. (2006). Parkin and defective ubiquitination in Parkinson's disease. P. D. P. Riederer, P. D. H. Reichmann, P. D. M. B. H. Youdim, & P. D. M. Gerlach (Eds.). *Parkinson's Diseaseand Related Disorders*, 209–213.

Del Hoyo, P., García-Redondo, A., De Bustos, F., Molina, J. A., Sayed, Y., Alonso-Navarro, H., … Jiménez-Jiménez, F. J. (2010). Oxidative stress in skin fibroblasts cultures from patients with Parkinson's disease. *BMC Neurology*, *10*, 95.

Di Scala, C., Yahi, N., Boutemeur, S., Flores, A., Rodriguez, L., Chahinian, H., & Fantini, J. (2016). Common molecular mechanism of amyloid pore formation by Alzheimer's beta-amyloid peptide and alpha-synuclein.*Scientific Reports*, *6*, 28781.

Dimri, G. P., Lee, X., Basile, G., Acosta, M., Scott, G., Roskelley, C., … Campisi, J. (1995). A biomarker that identifies senescent human cells in culture and in aging skin in vivo. *Proceedings of the National Academy ofSciences of the United States of America*, *92*, 9363–9367.

Dodson, M. W., & Guo, M. (2007). Pink1, Parkin, DJ-1 and mitochondrialdysfunction in Parkinson's disease. *Current Opinion in Neurobiology*, *17*,331–337.

El-Hafidi, M., Meschini, M. C., Rizza, T., Santorelli, F. M., Bertini, E., Carrozzo, R., & Vàzquez-Memije, M. E. (2011). Cardiolipin content in mitochondria from cultured skin fibroblasts harboring mutations in the mitochondrial ATP6 gene. *Journal of Bioenergetics and Biomembranes*, *43*, 683–690.

Fabelo, N., Martín, V., Santpere, G., Marín, R., Torrent, L., Ferrer, I., & Diaz, M. (2011). Severe alterations in lipid composition of frontal cortex lipid rafts from Parkinson's disease and incidental Parkinson's disease. *Molecular Medicine (Cambridge, Mass.)*, *17*, 1107–1118.

Fallon, L., Moreau, F., Croft, B. G., Labib, N., Gu, W. J., & Fon, E. A. (2002). Parkin and CASK/LIN-2 associate via a PDZ-mediated interaction and are co-localized in lipid rafts and postsynaptic densities in brain. *Journalof Biological Chemistry*, *277*(1), 486–491.

Farmer, K., Smith, C. A., Hayley, S., & Smith, J. (2015). Major alterations of phosphatidylcholine and lysophosphatidylcholine lipids in the substan- tia nigra using an early stage model of Parkinson''s disease. *InternationalJournal of Molecular Sciences*, *16*, 18865–18877.

Ferretta, A., Gaballo, A., Tanzarella, P., Piccoli, C., Capitanio, N., Nico, B., … Cocco, T. (2014). Effect of resveratrol on mitochondrial function: Implications in parkin-associated familiar Parkinson's disease. *Biochi-mica et Biophysica Acta*, *1842*, 902–915.

Fuchs, B., Schiller, J., Süss, R., Schürenberg, M., & Suckau, D. (2007). A direct and simple method of coupling matrix-assisted laser desorption and ionization time-of-flight mass spectrometry (MALDI-TOF MS) to thin- layer chromatography (TLC) for the analysis of phospholipids from egg yolk. *Analytical and Bioanalytical Chemistry*, *389*, 827–834.

Fuller, M. (2010). Sphingolipids: The nexus between Gaucher disease andinsulin resistance. *Lipids in Health and Disease*, *9*, 113.

Gai, W. P., Yuan, H. X., Li, X. Q., Power, J. T., Blumbergs, P. C., & Jensen, P. H. (2000). In situ and in vitro study of colocalization and segregation of alpha-

synuclein, ubiquitin and lipids in Lewy bodies. *Experimental Neurology*, *166*, 324–333.

Gegg, M. E., Sweet, L., Wang, B. H., Shihabuddin, L. S., Sardi, S. P., & Schapira, A. H. (2015). No evidence for substrate accumulation in Parkinson brains with GBA mutations. *Movement Disorders*, *30*(8), 1085–1089.

Grünewald, A., Voges, L., Rakovic, A., Kasten, M., Vandebona, H., Hemmelmann, C., … Klein, C. (2010). Mutant parkin impairs mitochondrial function and morphology in human fibroblasts. *PLoS ONE*, *5*, e12962.

Grey, M., Dunning, C. J., Gaspar, R., Grey, C., Brundin, P., Sparr, E., & Linse, S. (2015). Acceleration of α-synuclein aggregation by exosomes. *TheJournal of Biological Chemistry*, *290*, 2969–2982.

Grimm, M. O. W., Tschäpe, J. A., Grimm, H. S., Zinser, E. G., & Hartmann, T. (2006). Altered membrane fluidity and lipid raft composition in presenilin-deficient cells. *Acta Neurologica Scandinavica Supplementum*, *185*, 27–32.

Hartmann, T., Kuchenbecker, J., & Grimm, M. O. W. (2007). Alzheimer'sdisease: The lipid connection. *Journal of Neurochemistry*, *103*(Suppl 1),159–170.

Hoepken, H. H., Gispert, S., Morales, B., Wingerter, O., Del Turco, D., Mülsch, A., … Auburger, G. (2007). Mitochondrial dysfunction, peroxidation damage and changes in glutathione metabolism inPARK6. *Neurobiology of Disease*, *25*(2), 401–411.

Ivatt, R. M., Sanchez-Martinez, A., Godena, V. K., Brown, S., Ziviani, E., & Whitworth, A. J. (2014). Genome-wide RNAi screen identifies the Parkinson disease GWAS risk locus SREBF1 as a regulator of mitophagy. *Proceedings of the National Academy of Sciences of the United States of America*, *111*(23), 8494–8499.

Jackson, S. N., Colsch, B., Egan, T., Lewis, E. K., Schultz, J. A., & Woods, A. S.(2011). Gangliosides' analysis by MALDI-ion mobility MS. *Analyst*, *136*,463–466.

Jin, S. M., & Youle, R. J. (2012). PINK-1 and Parkin-mediated mitophagy at aglance. *Journal of Cell Science*, *125*, 795–799.

Kates, M. (1986). *Techniques of lipidology*. Amsterdam: Elsevier.

Kim, K. J., Stevens, M. V., Hasina Akter, M., Rusk, S. E., Huang, R. J., Cohen, A., … Sack, M. N. (2011). Parkin is a lipid-responsive regulator of fat uptake in mice and mutant human cells. *Journal of Clinical Investigation*, *121*(9), 3701–3712.

Kitada, T., Asakawa, S., Hattori, N., Matsumine, H., Yamamura, Y., Minoshima, S., … Shimizu, N. (1998). Mutations in the parkin gene cause autosomal recessive juvenile parkinsonism. *Nature*, *392*, 605–608.

Kitada, T., Tomlinson, J. J., Ao, H. S., Grimes, D. A., & Schlossmacher, M. G. (2012). Considerations regarding the etiology and future treatment of autosomal recessive versus idiopathic Parkinson disease. *Current Treatment Options in Neurology*, *14*, 230–240.

Klein, C., & Schlossmacher, M. G. (2006). The genetics of Parkinson disease: Implications for neurological care. *Nature Clinical Practice Neurology*, *2*, 136–146.

Kubo, S. I., Kitami, T., Noda, S., Shimura, H., Uchiyama, Y., Asakawa, S., … Hattori, N. (2001). Parkin is associated with cellular vesicles. *Journal of Neurochemistry*, *78*(1), 42–54.

Lee, J. Y., Nagano, Y., Taylor, J. P., Lim, K. L., & Yao, T. P. (2010). Disease- causing mutations in parkin impair mitochondrial ubiquitination, aggregation and HDAC6-dependent mitophagy. *The Journal of Cell Biology*, *189*, 671–679.

Lippolis, R., Siciliano, R. A., Pacelli, C., Ferretta, A., Mazzeo, M. F., Scacco, S., … Cocco, T. (2015). Altered protein expression pattern in skin fibroblasts from parkin-mutant early-onset Parkinson's disease pa- tients. *Biochimica et Biophysica Acta*, *1852*, 1960–1970.

Lwin, A., Orvisky, E., Goker-Alpan, O., LaMarca, M. E., & Sidransky, E. (2004). Glucocerebrosidase mutations in subjects with parkinsonism. *Molecular Genetics and Metabolism*, *81*, 70–73.

Mahyran, D. J. (1999). Biochemical consequences of mutations causing the GM2 gangliosidoses. *Biochimica et Biophysica Acta*, *1455*, 105–138.

Martin, D. R., Cox, N. R., Morrison, N. E., Kennamer, D. M., Peck, S. L., Dodson, A. N., … Baker, H. J. (2005). Mutation of the GM2 activator protein in a feline model of GM2 gangliosidosis. *Acta Neuropathologica*,*110*, 443–450.

Mata, I. F., Samii, A., Schneer, S. H., Roberts, J. W., Griffith, A., Leis, B. C., … Zabetian, C. P. (2008). Glucocerebrosidase gene mutations: A risk factor for Lewy body disorders. *Archives of Neurology*, *65*, 379–382.

Mazzulli, J. R., Xu, Y. H., Sun, Y., Knight, A. L., McLean, P. J., Caldwell, G. A., … Krainc, D. (2011). Gaucher disease glucocerebrosidase and α- synuclein form a bidirectional pathogenic loop in synucleinopathies. *Cell*, *146*, 37–52.

Mielke, M. M., Maetzler, W., Haughey, N. J., Bandaru, V. V., Savica, R., Deuschle, C., … Liepelt-Scarfone, I. (2013). Plasma ceramide and glucosylceramide metabolism is altered in sporadic Parkinson's disease and associated with cognitive impairment: A pilot study. *PLoS ONE*, *8*(9),e73094.

Mortiboys, H., Thomas, K. J., Koopman, W. J. H., Klaffke, S., Abou-Sleiman, P., Olpin, S., … Bandmann, O. (2008). Mitochondrial function and morphology are impaired in parkin-mutant fibroblasts. *Annals of Neurology*, *64*, 555–565.

Neumann, J., Bras, J., Deas, E., O'Sullivan, S. S., Parkkinen, L., Lachmann, R. H., … Wood, N. W. (2009). Glucocerebrosidase mutations in clinicaland pathologically proven Parkinson's disease. *Brain*, *132*, 1783–1794.

Pacelli, C., De Rasmo, D., Signorile, A., Grattagliano, I., Di Tullio, G., D'Orazio, A., … Cocco, T. (2011). Mitochondrial defect and PGC-1α dysfunction in parkin-associated familial Parkinson's disease. *Biochi-mica et Biophysica Acta*, *1812*, 1041–1053.

Piccinini, M., Scandroglio, F., Priori, S., Buccinnà, B., Loberto, N., Aureli, M., … Prinetti, A. (2010). Deregulated sphingolipid metabolism and membrane organization in neurodegenerative disorders. *Molecular Neurobiology*, *41*(2–3), 314–340.

Polymeropoulos, M. H., Lavedan, C., Leroy, E., Ide, S. E., Dehejia, A., Dutra, A., … Nussbaum, R. L. (1997). Mutation in the alpha-synuclein geneidentified in families with Parkinson's disease. *Science*, *276*, 2045–2047.

Qin, L., Wu, X., Block, M. L., Liu, Y., Breese, G. R., Hong, J. S., … Crews, F. T. (2007). Systemic LPS causes chronic neuroinflammation and progres- sive neurodegeneration. *Glia*, *55*, 453–462.

Rothfuss, O., Fischer, H., Hasegawa, T., Maisel, M., Leitner, P., Miesel, F., … Patenge, N. (2009). Parkin protects mitochondrial genome integrity and supports

mitochondrial DNA repair. *Human Molecular Genetics*, *18*, 3832–3850.

Sandebring, M. A., & Cedazo-Minguez, A. (2012). Parkin-an E3 ubiquitin ligase with multiple substrates. *Journal of Alzheimers Disease & Parkinsonism*, *S10*, 002.

Schöndorf, D. C., Aureli, M., McAllister, F. E., Hindley, C. J., Mayer, F., Schmid, B., … Deleidi, M. (2014). IPSC-derived neurons from GBA1-associated Parkinson's disease patients show autophagic defectsand impaired calcium homeostasis. *Nature Communications*, *5*, 4028.

Shimura, H., Hattori, N., Kubo, S., Yoshikawa, M., Kitada, T., Matsumine, H., … Mizuno, Y. (1999). Immunohistochemical and subcellular localization of Parkin protein: Absence of protein in autosomalrecessive juvenile parkinsonism patients. *Annals of Neurology*, *45*(5), 668–672.

Shimura, H., Hattori, N., Kubo, S., Mizuno, Y., Asakawa, S., Minoshima, S., … Suzuki, T. (2000). Familial Parkinson disease gene product, parkin, is a ubiquitin-protein ligase. *Nature Genetics*, *25*, 302–305.

Sidransky, E., & Lopez, G. (2012). The link between the GBA gene and parkinsonism. *Lancet Neurology*, *11*, 986–998.

Simons, K., & Toomre, D. (2000). Lipid rafts and signal trasduction. *Nature Reviews Molecular Cell Biology*, *1*(1), 31–39.

Simpson, M. A., Cross, H., Proukakis, C., Priestman, D. A., Neville, D. C. A., Reinkensmeier, G., … Crosby, A. H. (2004). Infantile-onset symptom- atic epilepsy syndrome caused by a homozygous loss-of-function mutation of GM3 synthase. *Nature Genetics*, *36*, 1225–1229.

Spillantini, M. G., Schmidt, M. L., Lee, V. M., Trojanowski, J. Q., Jakes, R., & Goedert, M. (1997). Alpha-synuclein in Lewy bodies. *Nature*, *388*, 839–840.

Sun, G., Yang, K., Zhao, Z., Guan, S., Han, X., & Gross, R. W. (2008). Matrix- assisted laser desorption/ionization-time of flight mass spectrometric analysis of cellular glycerophospholipids enabled by multiplexedsolvent dependent analyte-matrix interactions. *Analytical Chemistry*, 807576–807585.

Valente, E. M., Arena, G., Torosantucci, L., & Gelmetti, V. (2012). Molecular pathways in sporadic PD. *Parkinsonism and Related Disorders*, *18*, S71–S73.

Vergara, D., Ferraro, M. M., Cascine, M., Del Mercato, L. L., Leporatti, S., Ferretta, A., … Gaballo, A. (2014). Cytoskeletal alterations and biomechanical properties of parkin-mutant human primary fibroblasts. *Cell Biochemistry and Biophysics*, *71*(3), 1395–1404.

Vitale, R., Angelini, R., Lobasso, S., Capitanio, G., Ludwig, B., & Corcelli, A. (2015). MALDI-TOF/MS lipid profiles of cytochrome c oxidases: Cardiolipin is not an essential component of the Paracoccus denitrificans oxidase. *Biochemistry*, *54*(4), 1144–1150.

Xiong, H., Wang, D., Chen, L., Choo, Y. S., Ma, H., Tang, C., … Zhang, Z. (2009). Parkin, PINK1, and DJ-1 form a ubiquitin E3 ligase complex promoting unfolded protein degradation. *The Journal of Clinical Investigation*, *119*, 650–660.

Youle, R. J., & Narendra, D. P. (2011). Mechanisms of mitophagy. *NatureReviews Molecular Cell Biology*, *12*, 9–14.

Yu, R. K., Nakatani, Y., & Yanagisawa, M. (2008). The role of glycosphingolipid metabolism in the developing brain. *Journal of Lipid Research*, *50*, S440–S445.